Cell Calcium 83 (2019) 102058

Contents lists available at ScienceDirect

Cell Calcium

journal homepage: www.elsevier.com/locate/ceca

Extracellular calcium stimulates osteogenic differentiation of human adipose-derived stem cells by enhancing bone morphogenetic protein-2 expression

Risa Yanai[a], Fumi Tetsuo[b,h], Shinichi Ito[c], Momoe Itsumi[d], Junko Yoshizumi[e], Tomoko Maki[f], Yoshihide Mori[a], Yasutaka Kubota[g,*], Shunichi Kajioka[h,**]

[a] Department of Oral and Maxillofacial Surgery, Graduate School of Dental Science, Kyushu University, Japan
[b] Department of Periodontology Division of Oral Rehabilitation, Graduate School of Dental Science, Kyushu University
[c] Section of Dentistry, Fukuoka Tokushukai Medical Center, Japan
[d] Department of Oral Microbiology and Immunology, Showa University School of Dentistry, Japan
[e] Department of Oral and Maxillofacial Surgery, Fukuoka Dental College, Japan
[f] Section of Urology, Spinal Injuries Center, Japan
[g] Department of Oral and Maxillofacial Surgery, Sasebo Kyosai Hospital, Nabasaki, Japan
[h] Department of Clinical Pharmacology, Graduate School of Medical Sciences, Kyushu University, Japan

ARTICLE INFO

Keywords:
Human adipose-derived stem cells
BMP-2
Osteogenic
Extracellular Ca^{2+}

ABSTRACT

Bone morphogenetic protein-2 (BMP-2) promotes the differentiation of non-osteogenic mesenchymal cells to osteogenic cells. In this study, we isolated human adipose-derived stem cells (hASCs) and investigated the effects of recombinant human BMP-2 (rhBMP-2) and extracellular Ca^{2+} concentration ($[Ca^{2+}]_{out}$) on the osteogenic differentiation of hASCs. rhBMP-2 promoted calcium deposition in hASCs and stimulated the mRNA expressions of six proteins known to be involved in the osteogenic differentiation of hASCs: Runx2, osterix, alkaline phosphatase, osteonectin, bone sialoprotein and osteocalcin. Elevation of $[Ca^{2+}]_{out}$ enhanced the level of alkaline phosphatase enzyme, increased the mRNA expressions of Runx2 and osteocalcin and induced the expressions of BMP-2 mRNA and protein in hASCs. Elevation of $[Ca^{2+}]_{out}$ transiently increased the intracellular Ca^{2+} concentration ($[Ca^{2+}]_{in}$) due to activation of the calcium-sensing receptor (CaSR). The Ca^{2+}-induced expressions of BMP-2 mRNA and protein were inhibited by the calmodulin antagonist, W-7. Furthermore, elevation of $[Ca^{2+}]_{out}$ decreased the cytoplasmic level of phosphorylated nuclear factor of activated T-cell-2 (NFAT-2) and increased the nuclear level of dephosphorylated NFAT2. Taken together, these results suggest that rhBMP-2 promotes the osteogenic differentiation of hASCs. Furthermore, an increase in $[Ca^{2+}]_{out}$ enhances the expression of BMP-2 *via* activation of the CaSR, elevation of $[Ca^{2+}]_{in}$ and stimulation of Ca^{2+}/calmodulin-dependent NFAT-signaling pathways.

1. Introduction

Adipose-derived stem cells (ASCs) have high multi-differentiative potential [1,2]. ASCs retain their multipotency when expanded in culture and can differentiate into a variety of cell types, including osteoblasts, chondrocytes, myocytes and adipocytes [3]. Both autologous ASCs [4] and autologous bone marrow-derived mesenchymal stem cells (BMSCs) [5] have been used successfully for osteoregeneration in patients with critical bone defects. However, ASCs can be obtained easily from adipose tissue and with a greater cellular yield than BMSCs [6].

Bone morphogenetic proteins (BMPs) are members of the transforming growth factor-β superfamily of polypeptides. BMPs bind to the transmembrane heterotetrameric complexes formed by BMP receptor type IA (BMPR1A), type IB (BMPR1B) and type II (BMPR2). BMPs have unique functions in bone growth, including embryonic skeletal development [7] and postnatal bone remodeling [8]. Among the BMP family members, BMP-2 has been shown to stimulate osteogenic differentiation of mesenchymal progenitor cells [9]. Furthermore, exogenous

* Corresponding author at: Department of Oral and Maxillofacial Surgery, Sasebo Kyosai Hospital, 10-17 Shimanji-Cho, Sasebo, Nagasaki, 857-8575, Japan.
** Corrsponding author at: Department of Clinical Pharmacology, Graduate School of Medical Sciences, Kyushu University, 3-1-1 Maidashi Higashiku, Fukuoka, 812-8582, Japan.
E-mail addresses: kbt0830@yahoo.co.jp (Y. Kubota), kajioka@uro.med.kyushu-u.ac.jp (S. Kajioka).

https://doi.org/10.1016/j.ceca.2019.102058
Received 8 August 2018; Received in revised form 19 June 2019; Accepted 16 July 2019
Available online 08 August 2019
0143-4160/

application of BMP-2 also promotes the trans-differentiation of non-osteogenic mesenchymal cells, such as myogenic cells [10], fibroblasts [11] and ASCs [12], to osteogenic cells. Therefore, BMP-2 has attracted attention as a potential therapeutic agent, and recombinant human BMP-2 (rhBMP2) has been used to treat degenerative lumbar disc disease and tibial fractures [13]. However, the use of rhBMP-2 in the clinical setting could be problematic due to its high cost and potential risks of antigenicity and viral infection.

Changes in intracellular calcium level ($[Ca^{2+}]_{in}$) act as a universal signal that intersects with many pathways regulating gene expression [14]. Elevated $[Ca^{2+}]_{in}$ activates the phosphatase, calcineurin, by interacting with Ca^{2+}/calmodulin [15], and in turn, activated calcineurin dephosphorylates a set of substrates that include nuclear factor of activated T-cells (NFAT) [16]. Dephosphorylated NFAT translocates from the cytoplasm to the nucleus [17] and activates gene expression in cooperation with other transcriptional regulators [18]. NFATs are a family of four transcription factors, NFAT1, NFAT2, NFAT3 and NFAT4. Reportedly, NFAT2 regulates bone mass by affecting both osteoblasts and osteoclasts [19]. Furthermore, elevated $[Ca^{2+}]_{in}$ induces chondrogenesis in mesenchymal cells by stimulating BMP-2 expression *via* a calcineurin/NFAT pathway [20]. Although there is substantial evidence for the importance of $[Ca^{2+}]_{in}$ in the regulation of gene expression, the role of $[Ca^{2+}]_{in}$ in ASCs remains to be investigated.

The aim of this study was to examine how BMP-2 and Ca^{2+} regulate osteogenic differentiation in isolated human ASCs (hASCs) and determine whether Ca^{2+}/NFAT2 signaling pathways might contribute to the underlying mechanisms. To achieve this aim, we manipulated $[Ca^{2+}]_{in}$ in hASCs by varying extracellular Ca^{2+} concentration ($[Ca^{2+}]_{out}$), which has been shown in fibroblasts to influence $[Ca^{2+}]_{in}$ *via* a calcium-sensing receptor (CaSR) [21]. The osteogenic differentiation of hASCs was assessed by measuring the expressions of two transcription factors involved in osteoblastic differentiation, namely runt-related transcription factor-2 (Runx2) and osterix [22–24], as well as several bone proteins secreted by osteoblasts, namely osteonectin, osteocalcin, alkaline phosphatase (ALP) and bone sialoprotein (BSP) [23,25,26].

2. Materials and methods

2.1. hASC isolation and culture

hASCs were isolated according to the modified protocol of Zuk et al. [1]. Briefly, abdominal subcutaneous adipose tissue was collected from 11 patients (6 males and 5 females; mean age, 69.1 ± 11.5 years) admitted to Kyushu University Hospital, Japan. The Ethics Committee of Kyushu University approved the study protocol (No. 2019-130), and informed consent was obtained from all patients. The adipose tissues were minced into small pieces and washed extensively with sterile phosphate-buffered saline (PBS) to remove contaminating debris and red blood cells. The tissue fragments were digested by 0.075% type I collagenase (Worthington Biochemical Co., Lakewood, NJ, USA) in PBS for 60 min at 37 °C and centrifuged at 1500 rpm for 5 min to yield the stromal and vascular fractions (SVFs) and undigested tissue. The SVFs were resuspended in 160 mM NH_4Cl (Wako Pure Chemical Industries Ltd., Osaka, Japan) and filtered through membranes with 40-μm pores. After centrifugation at 1500 rpm for 5 min, the pellet was resuspended in Dulbecco's Modified Eagle Medium (DMEM; Sigma-Aldrich, St. Louis, MO, USA) containing 10% fetal bovine serum (FBS; ICN Biomedicals, Aurora, OH, USA), 100 U/mL penicillin and 100 μg/mL streptomycin (Wako Pure Chemical Industries Ltd), and the cells were cultured under a 95% air, 5% CO_2 atmosphere at 37 °C for 48–72 h. After the removal of nonadherent cells with PBS, the adherent cells were cultured to 80–90% confluence and used as hASCs. The hASCs were cultured in osteogenic differentiation medium (ODM) containing DMEM, 15% FBS, 0.1 μM dexamethasone (Sigma-Aldrich), 10 mM β-glycerol phosphate (Sigma-Aldrich), 50 μM L-ascorbic acid (Wako Pure Chemical Industries Ltd), 100 U/mL penicillin, 100 μg/mL streptomycin and various concentrations of Ca^{2+} [27].

2.2. Extraction of cytoplasmic and nuclear proteins

Cytoplasmic and nuclear proteins were extracted from cultured cells using a ProteoExtract® Subcellular Proteome Extraction kit (Merck, Darmstadt, Germany) according to the manufacturer's instructions.

2.3. Alizarin red S staining

Cells were cultured on 35-mm plates for 3, 7 or 14 days and then stained with Alizarin red S (Sigma-Aldrich) for 15 min [28]. Densitometric analysis of the staining was performed using ImageJ 1.48 [29].

2.4. von Kossa staining

Cells were cultured on chamber slides to reach 80% confluence. After stimulation with rhBMP-2 (R&D Systems Inc., Minneapolis, MN, USA) for 3, 7 or 14 days, the cells were stained with a calcium-staining kit (ScyTek Laboratories, Inc., West Logan, UT, USA) according to the manufacturer's instructions. Briefly, after fixation in 10% formalin, the cells were incubated first with 5% silver nitrate solution under ultraviolet light for 1 h and then with Nuclear Fast Red solution (Sigma-Aldrich) for 5 min to remove unreacted silver. The cells were washed with 100% ethanol. Densitometric analysis of the staining was performed using ImageJ 1.48.

2.5. ALP staining

ALP staining was performed after 3, 14 and 21 days of cell culture. Briefly, the cells were fixed in 10% formalin for 2 min and then incubated with ALP staining solution (Takara Bio, Shiga, Japan) for 15 min.

2.6. ALP activity

ALP activity was measured using an ALP assay kit (Wako Pure Chemical Industries) in accordance with the manufacturer's instructions. Briefly, cells were cultured in 48-well culture plates (3×10^4 cells/well) and lysed with 0.1% (v/v) Triton-X100. The cell lysates (20 μL) were incubated with 100 μL of a solution of the ALP substrate, p-nitrophenol phosphate, at 37 °C for 15 min. The reaction was stopped by the addition of 50 μL of 0.2 M NaOH, and the absorbance at 405 nm was measured [28].

2.7. Real-time polymerase chain reaction (qPCR)

Total RNA was isolated from cells using Trizol reagent (Invitrogen, Carlsbad, CA, USA) as described previously [21]. First-strand cDNA was synthesized from 3 μg total RNA, and qPCR was performed using specific primers. The primer sequences for the human genes encoding Runx2, osterix, osteonectin, BSP, osteocalcin, BMP-2, calcineurin and β-actin were as follows (forward/reverse): Runx2, CACAAGGACAGAGT CAGATTACA/ACGTCATCTGGCTCAGGTAG; osterix, ACGTCATCTGGC TCAGGTAG/CCTGCTTTGCCCAGAGTTGTTGA; osteonectin, GCTCAAG AACGTCCTGGTCA/TTCTCATGGATCTTCTTCAC; BSP, GGTATACAGG GTTAGCTGCAATC/TGGTACTGGTGCCGTTTATG; osteocalcin, CACAC TCCTCGCCCTATTG/GCACCTTTGCTGGACTCTG; BMP-2, CCCTACATG CTAGACCTGTATCG/TCCTCCGTGGGGATAGAAC; calcineurin, GTTTT CAGTGGACCCAGGAG/TGAAACTGTCGTACACCTTGAA; and β-actin, GCAAAGACCTGTACGCCAAC/CTAGAAGCGTTTGCGGTGGA. The mRNA levels were measured in triplicate using a qPCR system and the Brilliant SYBR Green qPCR kit (Stratagene, La Jolla, CA, USA). The PCR cycling conditions were: 10 min at 95 °C for 1 cycle followed by 45 cycles at 95 °C for 10 s, 60 °C for 30 s and 72 °C for 60 s. Dissociation

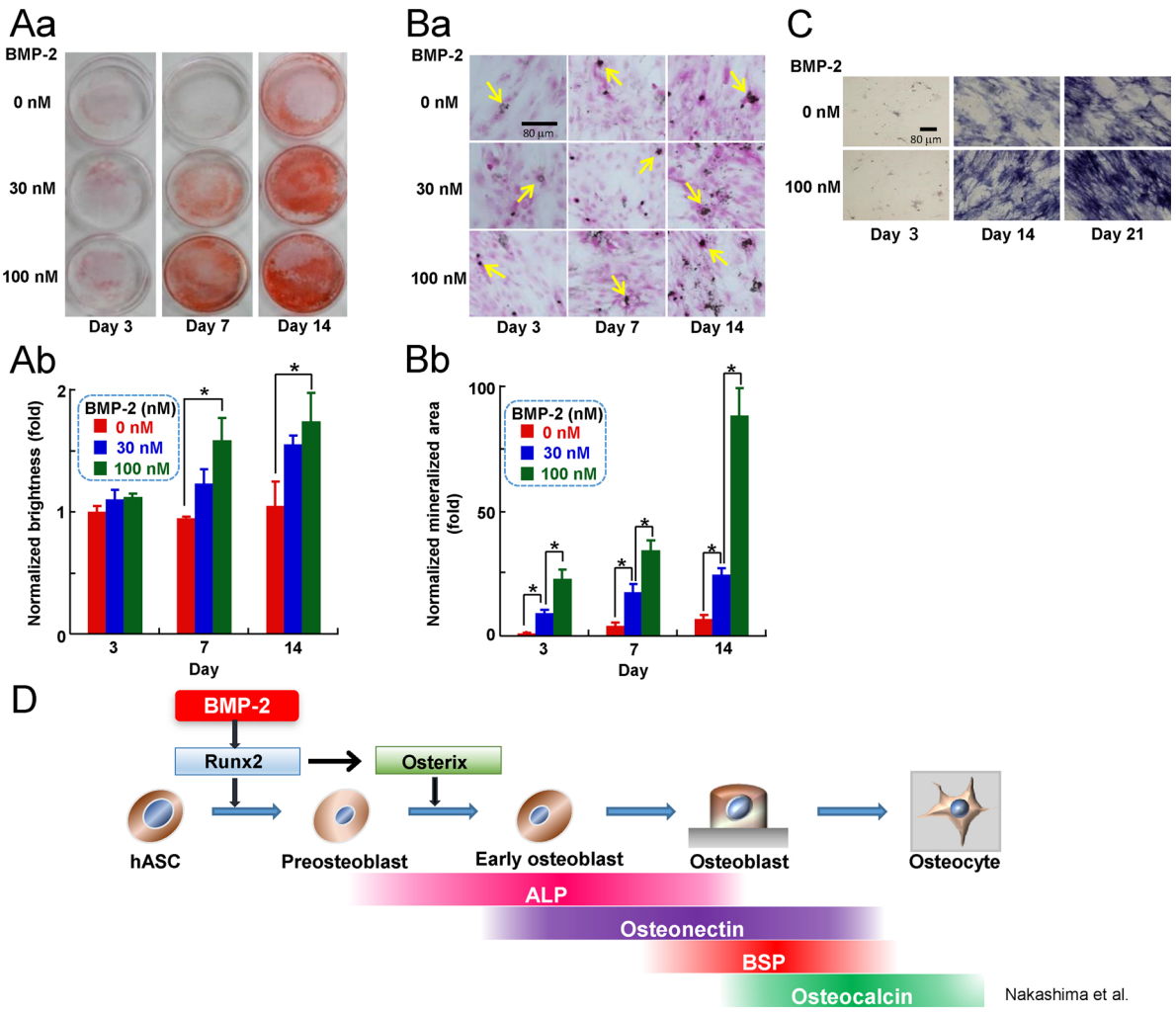

(caption on next page)

Fig. 1. Effects of recombinant human bone morphogenetic protein-2 (rhBMP-2) on calcium deposition in human adipose-derived stem cells (hASCs).
Calcium deposition in hASCs was analyzed by Alizarin red staining **(Aa, Ab)** and von Kossa staining **(Ba, Bb)**. hASCs were cultured in the absence or presence of rhBMP-2 (30 nM or 100 nM) for 3, 7 or 14 days and then stained with Alizarin red **(Aa, Ab)**. Bone nodules (punctate brown-colored staining) are indicated by the yellow arrows **(Ba)**. Densitometric analyses of Alizarin red staining **(Ab)** and mineralized area **(Bb)** in the absence or presence of rhBMP-2 (30 nM or 100 nM) at days 3, 7 and 14. The densities in **(Ab)** and **(Bb)** were normalized to that at day 3 in the absence of rhBMP-2. Vertical bars indicate the means ± standard deviations ($n = 4$). * $P < 0.05$. **(C)** hASCs cultured in the absence or presence of rhBMP-2 (100 nM) were stained for alkaline phosphatase (ALP) at days 3, 14 and 21. **(D)** Schematic figure illustrating the temporal pattern of the involvement of bone morphogenetic protein-2 (BMP-2), runt-related transcription factor-2 (Runx2), osterix, ALP, osteonectin, bone sialoprotein (BSP) and osteocalcin in the differentiation of hASCs to osteocytes. **(E)** Effect of rhBMP-2 on the mRNA expressions of various ossification-related proteins (Runx2, osterix, ALP, osteonectin [ON], BSP and osteocalcin [OC]) in hASCs at various time points (0, 3, 7, 10, 14 and 21 days of culture). The mRNA levels were measured using real-time polymerase chain reaction. The amount of each mRNA was normalized to that of β-actin and expressed relative to that in unstimulated cells in medium containing 1.8 mM Ca^{2+} at day 0. Vertical bars indicate the means ± standard deviations ($n = 4$). * $P <$ 0.05.

curve analyses confirmed that the signals corresponded to unique amplicons. The relative amount of mRNA was calculated by normalization to that of β-actin.

2.8. Western blot

Samples were suspended in sodium dodecyl sulfate (SDS) sample buffer (Bio-Rad, Hercules, CA, USA) as described previously [21]. Next, the samples were run on 12% SDS polyacrylamide gels and transferred onto nitrocellulose paper (Bio-Rad). After incubation with the primary antibody, protein bands were visualized using horseradish peroxidase-conjugated secondary antibodies and Enhanced Chemiluminescence Reagent (Amersham Pharmacia Biotech Inc., Piscataway, NJ, USA). The following primary antibodies were used: monoclonal antibodies against human Runx2 (R&D Systems Inc.), human osterix (R&D Systems Inc.), human osteocalcin (R&D Systems Inc.), human osteonectin (TaKaRa Bio, Shiga, Japan), human NFAT2 (Abcam, Cambridge, UK) and human phospho-NFAT2 (Abcam) and polyclonal antibodies against human ALP (R&D Systems Inc.) and human BSP (Millipore, Billerica, MA, USA). The bands were scanned using computer-assisted densitometry (ChemiDoc XRS-*J*; Bio-Rad) and analyzed using Quantity One software (Bio-Rad).

2.9. Enzyme-linked immunosorbent assay (ELISA) for BMP-2

Bovine BMP-2 and human BMP-2 concentrations were measured using ELISA kits (TSZ ELISA, Framingham, MA, USA and R&D Systems Inc., respectively) in accordance with the manufacturer's instructions. Standard curves were generated using serial dilutions of standard recombinant bovine BMP-2 and human BMP-2 samples. The absorbance was measured at 450 nm [30].

2.10. $[Ca^{2+}]_{in}$ imaging

Relative $[Ca^{2+}]_{in}$ was measured using fluo-4 as described previously [20]. Briefly, hASCs were cultured on coverslips and incubated with 30 μM fluo-4 acetoxymethyl ester (fluo-4-AM) for 30 min. Coverslips with ASCs were placed in a perfusion chamber and washed with HEPES-buffered saline (140 mM NaCl, 5 mM KCl, 1 mM $MgCl_2$, 1 mM Na_2HPO_4, 10 mM glucose and 10 mM HEPES, pH 7.4). The cells were stimulated with HEPES-buffered saline containing various concentrations of $CaCl_2$ ($[Ca^{2+}]_{out}$). Fluo-4 fluorescence images (emission, 530 nm) of the cells were recorded every 1.7425 s, and the fluo-4 fluorescence (F) intensities were captured by a computer system. The fluo-4 fluorescence value relative to that at 0 mM Ca^{2+} (F_0) was calculated as $(F - F_0)/F_0$.

2.11. Statistical analyses

All data are presented as the mean ± standard deviation (SD). An unpaired *t*-test was used for statistical comparisons between experimental groups. A *P*-value < 0.05 was considered to indicate statistical significance.

3. Results

3.1. Effects of BMP-2 on the osteogenic differentiation of hASCs

To investigate the effects of BMP-2 on the osteogenic differentiation of hASCs, calcium deposition in the cells was investigated using the Alizarin red staining technique. hASCs were cultured in ODM containing 1.8 mM Ca^{2+}, and Alizarin red staining was performed at days 3, 7 and 14. hASCs cultured in the absence of rhBMP-2 (0 nM) failed to show a significant increase in calcium deposition. By contrast, hASCs cultured in the presence of 100 nM rhBMP-2 displayed a significant enhancement of calcium deposition compared to those cultured without rhBMP-2 at day 7 (1.5 ± 0.2-fold; $n = 4$) and day 14 (1.6 ± 0.2-fold; $n = 4$; Fig. 1Aa & 1Ab). Although there was a trend toward greater calcium deposition in cells cultured in 30 nM rhBMP-2, statistical significance was not reached (Fig. 1Ab).

The mineralization of hASCs in culture was further examined using the von Kossa staining technique. Representative images of hASCs cultured without and with 30 and 100 nM BMP-2 at days 3, 7 and 14 are shown in Fig. 1Ba. BMP-2 caused a concentration- and time-dependent increase in the mineralization of hASCs (30 nM BMP-2: 4.0 ± 1.3-fold at day 3, 17.4 ± 3.3-fold at day 7 and 34.2 ± 4.2-fold at day 14; 100 nM BMP-2: 6.7 ± 1.8-fold at day 3, 24.5 ± 2.7-fold at day 7 and 88.2 ± 11.2-fold at day 14; values are normalized to those in the absence of rhBMP-2 at day 3; $n = 4$ each; Fig. 1Ba & 1Bb). Representative images of hASCs cultured without and with 30 and 100 nM BMP-2 and stained with the ALP staining technique are shown in Fig. 1C; the stimulation of mineralization by 100 nM BMP-2 is clearly evident.

Runx2 and osterix are important transcription factors required during the early stage of the differentiation process (Fig. 1D) [22,23]. Therefore, we next examined how BMP-2 affected the expressions of Runx2 and osterix. When hASCs were cultured in ODM containing 1.8 mM Ca^{2+}, Runx2 mRNA expression showed a transient increase at day 3 (Fig. 1E), and this increase was potentiated by 100 nM BMP-2 (7.7 ± 0.1-fold, $n = 4$) but not 30 nM BMP-2 (Fig. 1E). Unlike Runx2 mRNA, osterix mRNA displayed a gradual increase in its expression level from day 10 (Fig. 1E). Furthermore, the expression of osterix mRNA was enhanced by 100 nM BMP-2 from day 10 onwards (15.1 ± 1.3-fold at day 10, $n = 4$; Fig. 1E), although 30 nM BMP-2 was without significant effect (Fig. 1E).

Subsequently, we investigated the expression profiles of ALP, osteonectin, BSP and osteocalcin (Fig. 1E) in the presence of 0, 30 or 100 nM BMP-2, since these factors are also important during the differentiation of hASCs into osteocytes (Fig. 1D) [23]. Osteonectin expression is generally observed during the later stages of differentiation [25], while BSP (an acidic, noncollagenous glycoprotein) and osteocalcin (a bone Gla protein) are both expressed in osteoblasts [26]. The level of ALP mRNA showed a continual increase over time from day 7 (Fig. 1E) and was potentiated specifically on day 10 by 100 nM BMP-2 (8.6 ± 1.4-fold, $n = 4$; Fig. 1E) but not 30 nM BMP-2. The expressions of osteonectin, BSP and osteocalcin increased from day 10 and were significantly enhanced by BMP-2 in a concentration-dependent manner (Fig. 1E): the maximal effect of 100 nM BMP-2 was observed at day 14 (osteonectin: 8.9 ± 1.1-fold, $n = 4$; BSP: 8.4 ± 0.4-fold, $n = 4$;

osteocalcin: 4.3 ± 0.1-fold, $n = 4$).

3.2. Effect of $[Ca^{2+}]_{out}$ on the osteogenic differentiation of hASCs

Manipulation of $[Ca^{2+}]_{out}$ has been suggested as a simple and economic method of priming human bone marrow-derived mesenchymal stromal cells for differentiation into bone tissue [31]. Thus, we examined whether $[Ca^{2+}]_{out}$ affected the osteogenic differentiation of hASCs. First, we compared the effects of various levels of $[Ca^{2+}]_{out}$ (0.3, 1.8 or 5.0 mM) with those of different concentrations of rhBMP-2 (0, 30 or 100 nM; in the presence of 0.3 mM $[Ca^{2+}]_{out}$) on cellular ALP activity (measured at days 0, 3, 7, 14 and 21). The level of ALP activity was measured as the concentration of p-nitrophenol formed as the reaction product in the assay. When hASCs were cultured for 21 days in ODM containing 0.3 mM Ca^{2+}, the p-nitrophenol concentration was significantly enhanced by rhBMP-2 from 0.3 ± 0.1 mM ($n = 4$) in the absence of rhBMP-2 to 0.8 ± 0.1 mM ($n = 4$; $P = 0.016$) in the presence of 30 nM rhBMP-2 and 1.3 ± 0.2 mM ($n = 4$; $P = 0.005$) in the presence of 100 nM rhBMP-2 (Fig. 2Aa). No significant effects of either concentration of rhBMP-2 were detected at earlier time points (Fig. 2Aa). Notably, elevating $[Ca^{2+}]_{out}$ from 0.3 mM to 1.8 mM or 5.0 mM (in the absence of rhBMP-2) also increased the p-nitrophenol concentration in cultured hASCs, with significant effects ($P < 0.05$) observed at 7, 14 and 21 days (Fig. 2Ab). At day 21, the p-nitrophenol concentration was significantly higher in hASCs cultured in 1.8 mM $[Ca^{2+}]_{out}$ (0.9 ± 0.1 mM; $n = 4$; $P = 0.0002$) or 5.0 mM $[Ca^{2+}]_{out}$ (1.3 ± 0.1 mM; $n = 4$; $P = 0.0004$) than in cells cultured in 0.3 mM $[Ca^{2+}]_{out}$ (0.3 ± 0.1; $n = 4$; Fig. 2Ab).

Next, we determined the effects of varying $[Ca^{2+}]_{out}$ on the mRNA expressions of Runx2 and osteocalcin. The transient up-regulation of Runx2 mRNA expression at day 3 was similar for $[Ca^{2+}]_{out}$ of 0.3 mM (5.0 ± 0.1-fold; $n = 4$) and 1.8 mM (4.2 ± 0.1-fold; $n = 4$) but was significantly augmented in the presence of 5.0 mM $[Ca^{2+}]_{out}$ (7.6 ± 0.04-fold; $n = 4$, $P = 0.002$; Fig. 2Ba). Osteocalcin mRNA expression in hASCs cultured in 0.3 mM $[Ca^{2+}]_{out}$ was increased at days 10, 14 and 21 (Fig. 2Bb), and this up-regulation of osteocalcin mRNA expression was enhanced by elevations in $[Ca^{2+}]_{out}$. For example, osteocalcin mRNA expression at day 21 was significantly higher in hASCs cultured in 1.8 mM $[Ca^{2+}]_{out}$ (4.2 ± 0.2-fold; $n = 4$, $P = 0.002$) or 5.0 mM $[Ca^{2+}]_{out}$ (4.3 ± 0.58-fold; $n = 4$, $P = 0.001$) than in cells cultured in 0.3 mM $[Ca^{2+}]_{out}$ (2.6 ± 0.3; $n = 4$; Fig. 2Bb).

The effects of elevating $[Ca^{2+}]_{out}$ on the expressions of Runx2 mRNA and osteocalcin mRNA mirrored those observed with BMP-2 (Fig. 1E). Therefore, we explored whether increasing $[Ca^{2+}]_{out}$ would enhance BMP-2 levels (Fig. 2Ca & 2Cb). Compared with that measured at 0.3 mM $[Ca^{2+}]_{out}$, the mRNA expression of BMP-2 was significantly enhanced ($P < 0.05$) at 1.8 mM $[Ca^{2+}]_{out}$ (3.0 ± 0.11-fold after 24 h, $n = 4$; 4.9 ± 0.07-fold after 48 h, $n = 4$) and 5.0 mM $[Ca^{2+}]_{out}$ (9.2 ± 0.61-fold after 24 h, $n = 4$; 9.3 ± 0.53-fold after 48 h, $n = 4$; Fig. 2Ca). Furthermore, $[Ca^{2+}]_{out}$ had a concentration-dependent effect on the level of BMP-2 protein in the culture medium measured at 48 h after priming the differentiation process (0.3 mM $[Ca^{2+}]_{out}$: 11.7 ± 2.9 pg/mL, $n = 4$; 1.8 mM $[Ca^{2+}]_{out}$: 25.0 ± 5.0 pg/mL, $n = 4$; and 5.0 mM $[Ca^{2+}]_{out}$: 45.0 ± 8.7 pg/mL, $n = 4$; Fig. 2Cb).

3.3. The roles of the CaSR and phospholipase C (PLC) in the mechanism linking $[Ca^{2+}]_{out}$ and $[Ca^{2+}]_{in}$ in hASCs

First, we assessed whether the CaSR was expressed in hASCs. Immunohistochemistry and western blotting experiments demonstrated the expression of CaSR protein in hASCs cultured for 10 days in ODM containing 5.0 mM $[Ca^{2+}]_{out}$ (Fig. 2Da & 2Db). There was a notable increase in the expression of CaSR mRNA at day 10, and this up-regulation of CaSR mRNA expression was almost doubled when the $[Ca^{2+}]_{out}$ was increased from 1.8 mM to 5.0 mM (Fig. 2E). By contrast, there were no significant changes in CaSR mRNA expression when hASCs were cultured for 10 days in ODM containing 0.3 mM $[Ca^{2+}]_{out}$ (data not shown). Subsequently, we examined whether CaSR activation might be linked to BMP-2 production. For these experiments, 1 μM R568 and 100 nM nifedipine were used as agonists of the CaSR and 1 μM NPS2143 was used as an antagonist (Fig. 2F). The BMP-2 protein level was 25.0 ± 5.0 pg/mL ($n = 4$) in ODM containing 1.8 mM $[Ca^{2+}]_{out}$ and was significantly elevated in the presence of a CaSR agonist (R568: 41.7 ± 5.6 pg/mL, $n = 4$, $P = 0.02$; nifedipine: 48.3 ± 5.8 pg/mL, $n = 4$, $P = 0.049$; Fig. 2F) and significantly reduced in the presence of a CaSR antagonist (NPS2143: 18.3 ± 2.9 pg/mL, $n = 4$, $P = 0.048$; Fig. 2F). Furthermore, when the CaSR was activated with 5.0 mM $[Ca^{2+}]_{out}$, the level of BMP-2 protein (45.0 ± 5.0 pg/mL, $n = 4$, $P = 0.004$) was similar to that seen in the presence of a CaSR agonist at 1.8 mM $[Ca^{2+}]_{out}$ (Fig. 2F). Taken together, these observations imply that activation of the CaSR promotes the production of BMP-2. Thus, activation of the CaSR by extracellular calcium would enhance the synthesis of BMP-2 and promote the osteogenic differentiation of hASCs.

Subsequently, we used Ca^{2+} imaging of hASCs loaded with fluo-4-AM to examine how $[Ca^{2+}]_{in}$ responded to changes in $[Ca^{2+}]_{out}$. When $[Ca^{2+}]_{out}$ was altered from 0 mM to 0.3 mM (Fig. 3A), there was very little change in the intracellular fluorescence level (representing $[Ca^{2+}]_{in}$). However, an obvious increase in the intracellular fluorescence level was observed when $[Ca^{2+}]_{out}$ was further elevated to 1.8 mM or 5.0 mM (this is clearly evident in the cell marked by the yellow arrowhead in Fig. 3A). $[Ca^{2+}]_{in}$ gradually increased when $[Ca^{2+}]_{out}$ was sequentially elevated from 0 mM to 0.3 mM, 1.8 mM and 5.0 mM, and this effect was reversible on the return of $[Ca^{2+}]_{out}$ to 0 mM (Fig. 3Ba). Furthermore, the application of 10 mM $[Ca^{2+}]_{out}$ was associated with a rapid but transient increase in $[Ca^{2+}]_{in}$, which may have been due to Ca^{2+} release from an intracellular Ca^{2+} store, followed by a sustained gradual elevation of $[Ca^{2+}]_{in}$ (Fig. 3Bb). A gradual increase in $[Ca^{2+}]_{in}$ was also observed when 100 nM nifedipine (a CaSR agonist) was applied (Fig. 3Ca), whereas a significant decrease in $[Ca^{2+}]_{in}$ occurred when 1 μM NSP2143 (a CaSR antagonist) was administered (Fig. 3Cb; note that one cell exhibited a transient spike in $[Ca^{2+}]_{in}$ at 1.8 mM $[Ca^{2+}]_{out}$). The effects of PLC on $[Ca^{2+}]_{in}$ were investigated using U-73122 as a pharmacologic inhibitor of PLC and U-73343 (an inactive analogue of U-73122) as a control. When U-73122 was applied, $[Ca^{2+}]_{in}$ decreased gradually, and the response to 5.0 mM $[Ca^{2+}]_{out}$ was impaired (Fig. 3D).

The effects of $[Ca^{2+}]_{out}$, nifedipine, NPS2143, U-73343 and U-73122 on the intracellular fluo-4 fluorescence level (used to reflect $[Ca^{2+}]_{in}$) are summarized in Fig. 3E. The intracellular fluo-4 fluorescence level was calculated as $(F - F_0)/F_0$, where F_0 is the background fluorescence level in 0 mM $[Ca^{2+}]_{out}$ and F is the fluorescence level under the indicated condition. An elevation of $[Ca^{2+}]_{out}$ resulted in a concentration-dependent increase in $[Ca^{2+}]_{in}$ as measured from the intracellular fluo-4 fluorescence level (0.3 mM $[Ca^{2+}]_{out}$: 0.28 ± 0.06, $n = 12$; 1 mM $[Ca^{2+}]_{out}$: 0.54 ± 0.04, $n = 12$; 1.8 mM $[Ca^{2+}]_{out}$: 0.63 ± 0.09, $n = 12$; 5.0 mM $[Ca^{2+}]_{out}$: 0.97 ± 0.13, $n = 12$; 10 mM $[Ca^{2+}]_{out}$: 0.97 ± 0.11, $n = 10$). 100 nM nifedipine in the presence of 1 mM $[Ca^{2+}]_{out}$ increased the intracellular fluo-4 fluorescence level (0.76 ± 0.07, $n = 10$, $P = 0.043$). By contrast, 1 μM NPS2143 and 1 nM U-73122 in the presence of 5.0 mM $[Ca^{2+}]_{out}$ significantly inhibited the intracellular fluo-4 fluorescence level (NPS2143: 0.42 ± 0.16, $n = 6$, $P = 0.042$; U-73122: 0.77 ± 0.22, $n = 5$, $P = 0.034$). In control experiments for U-73122, 1 nM U-73343 (which does not inhibit PLC) in the presence of 5.0 mM $[Ca^{2+}]_{out}$ had no effect on the intracellular fluo-4 fluorescence level (0.98 ± 0.26, $n = 5$).

3.4. Intracellular signaling mechanisms recruited by $[Ca^{2+}]_{in}$ to regulate the production of BMP-2 in hASCs

The remaining experiments were conducted using a $[Ca^{2+}]_{out}$ of 5 mM (unless otherwise noted), since the production of BMP-2 was

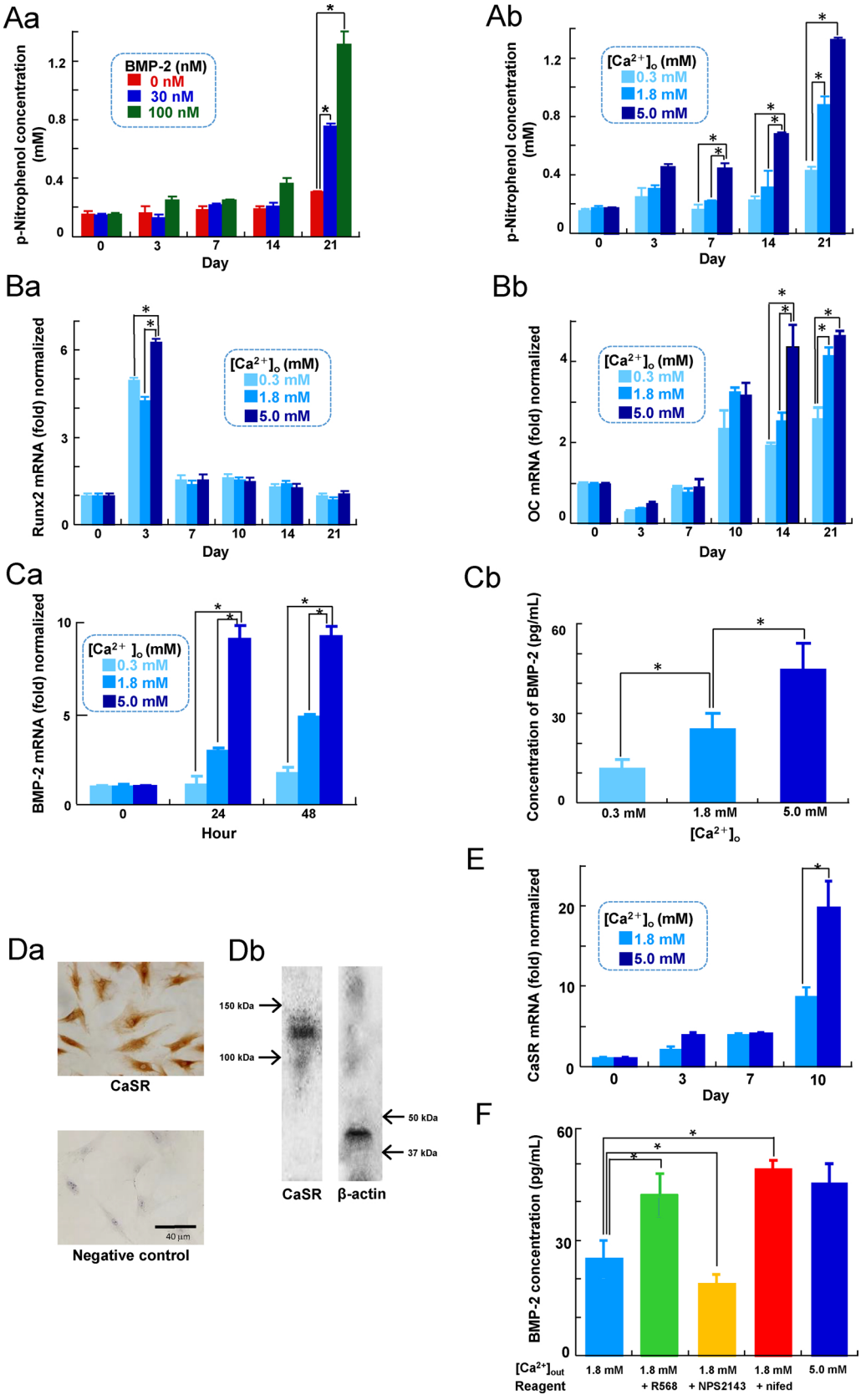

Fig. 2. Effects of extracellular calcium ion concentration ($[Ca^{2+}]_{out}$) on genes associated with osteogenic differentiation and the calcium-sensing receptor (CaSR) in human adipose-derived stem cells (hASCs).

(Aa) The effects of bone morphogenetic protein-2 (BMP-2; 0, 30 or 100 nM) on the level of alkaline phosphatase (ALP) activity in hASCs at various time points (0, 3, 7, 10, 14 or 21 days of culture). ALP activity was reflected by the concentration of p-nitrophenol produced by the assay. **(Ab)** The effects of various concentrations of $[Ca^{2+}]_{out}$ (0.3, 1.8 or 5.0 mM) on the level of ALP activity in hASCs at various time points (0, 3, 7, 10, 14 or 21 days of culture). **(Ba, Bb, Ca)** The effects of various concentrations of $[Ca^{2+}]_{out}$ (0.3, 1.8 or 5.0 mM) on the mRNA expression levels of Runx2 **(Ba)**, osteocalcin **(Bb)** and BMP-2 **(Ca)** in hASCs cultured in osteogenic differentiation medium for various time periods (0, 24 or 48 h). The mRNA levels were measured using real-time polymerase chain reaction (qPCR). The Runx2, osteocalcin and BMP-2 mRNA levels were normalized to that of β-actin and expressed relative to that in unstimulated cells in medium containing 0.3 mM Ca^{2+} at day 0. **(Cb)** BMP-2 concentration in hASCs cultured for 48 h in osteogenic differentiation medium containing 0.3, 1.8 or 5.0 mM $[Ca^{2+}]_{out}$. The BMP-2 concentration was measured using an enzyme-linked immunosorbent assay kit. **(Da)** Detection of CaSR protein in hASCs (cultured for 3 days) using immunohistochemistry techniques. The anti-CaSR antibody was omitted in the negative control. **(Db)** Detection of CaSR protein in hASCs (cultured for 3 days) using the western blot technique. **(E)** The effects of various $[Ca^{2+}]_{out}$ (1.8 or 5.0 mM) on the mRNA expression level of the CaSR in hASCs at different time points (0, 3, 7 or 10 days of culture). The mRNA level was measured using real-time polymerase chain reaction. The CaSR mRNA level was normalized to that of β-actin and expressed relative to that in unstimulated cells in medium containing 1.8 mM Ca^{2+} at day 0. **(F)** Summary of the effects of a CaSR antagonist (NPS2143) and two CaSR agonists (R568 and nifedipine) on the level of BMP-2 in hASCs cultured for 48 h. The BMP-2 protein concentration was measured using an enzyme-linked immunosorbent assay kit. Vertical bars indicate the means ± standard deviations ($n = 4$). * $P < 0.05$.

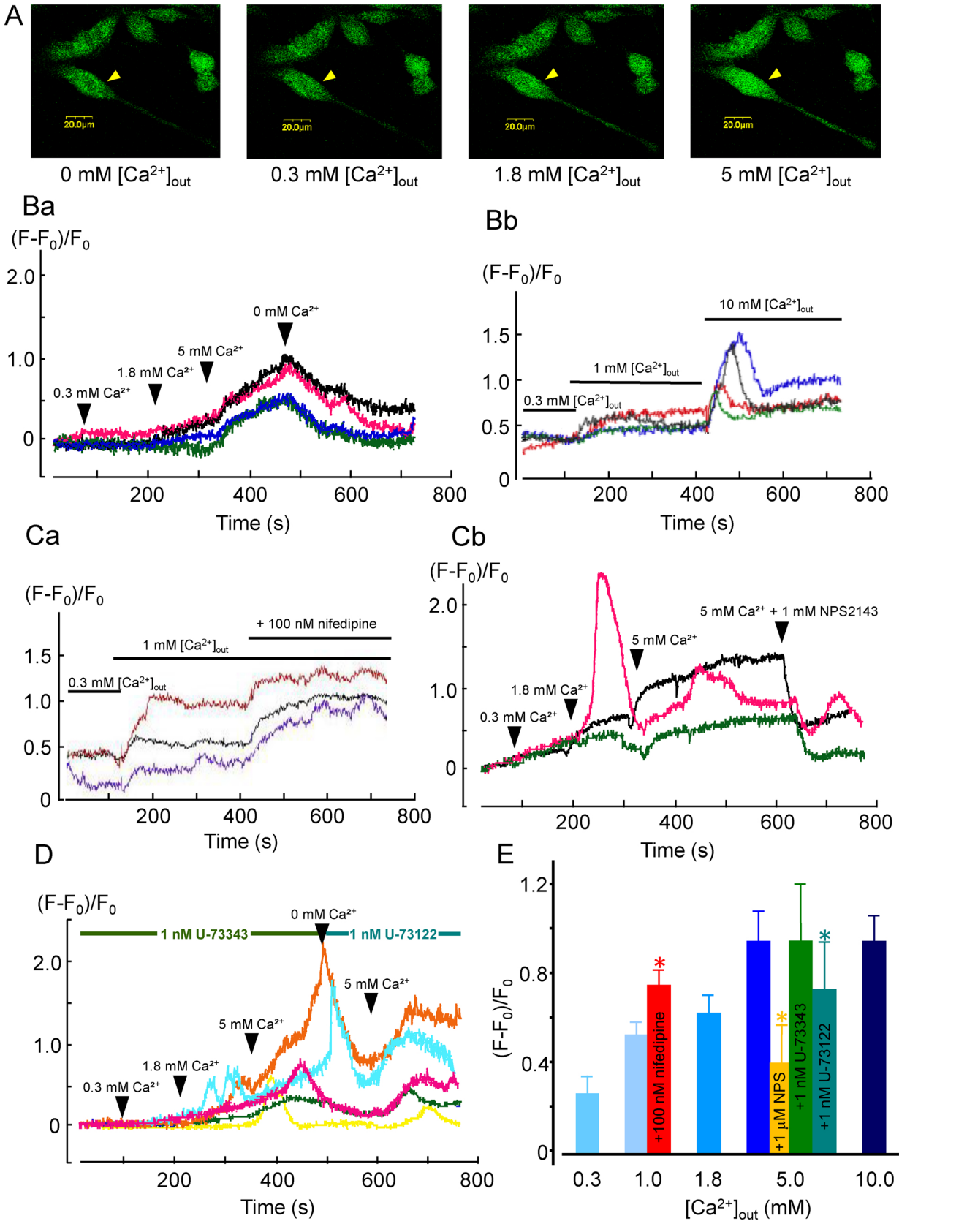

(caption on next page)

Fig. 3. The role of the calcium-sensing receptor (CaSR) in mediating the association between extracellular calcium ion concentration ($[Ca^{2+}]_{out}$) and intracellular calcium ion concentration ($[Ca^{2+}]_{in}$) in human adipose-derived stem cells (hASCs).
(A) Representative fluorescence microscopy images of a hASC loaded with fluo-4-acetoxymethyl ester (fluo-4-AM) and exposed to various $[Ca^{2+}]_{out}$ (nominally calcium-free [0 mM], 0.3 mM, 1.8 mM or 5.0 mM). **(Ba)** Each trace represents a real-time record of intracellular fluo-4 fluorescence (representing $[Ca^{2+}]_{in}$) in a different hASC loaded with fluo-4-AM and exposed to step-increases in $[Ca^{2+}]_{out}$ from nominally Ca^{2+}-free to 0.3 mM, 1.8 mM and then 5.0 mM. **(Bb)** Each trace represents a real-time record of intracellular fluo-4 fluorescence (representing $[Ca^{2+}]_{in}$) in a different hASC loaded with fluo-4-AM and exposed to step-increases in $[Ca^{2+}]_{out}$ from nominally Ca^{2+}-free to 1 mM and then 10 mM. **(Ca)** Each trace represents a real-time record of intracellular fluo-4 fluorescence (representing $[Ca^{2+}]_{in}$) in a different hASC loaded with fluo-4-AM and exposed first to 1 mM $[Ca^{2+}]_{out}$ and then to 100 nM nifedipine in the continued presence of 1 mM $[Ca^{2+}]_{out}$. **(Cb)** Each trace represents a real-time record of intracellular fluo-4 fluorescence (representing $[Ca^{2+}]_{in}$) in a different hASC loaded with fluo-4-AM and exposed to step-increases in $[Ca^{2+}]_{out}$ from nominally Ca^{2+}-free to 0.3 mM, 1.8 mM and 5.0 mM followed by 1 μM NPS2143 in the continued presence of 5.0 mM $[Ca^{2+}]_{out}$. **(D)** Each trace represents a real-time record of intracellular fluo-4 fluorescence (representing $[Ca^{2+}]_{in}$) in a different hASC loaded with fluo-4-AM. The cells were first exposed to step-increases in $[Ca^{2+}]_{out}$ from nominally Ca^{2+}-free to 0.3 mM, 1.8 mM and 5.0 mM in the continued presence of 1 nM U-73343. Subsequently, the cells were exposed to 1 nM U-73122 in the continued presence of 5.0 mM $[Ca^{2+}]_{out}$. **(E)** Summary of the results of the experiments shown in (Ba), (Bb), (Ca), (Cb) and (D). The intracellular fluo-4 fluorescence level was calculated as $(F - F_0)/F_0$, where F_0 is the background fluorescence level in 0 mM $[Ca^{2+}]_{out}$ and F is the fluorescence level under the indicated condition: 0.3 mM $[Ca^{2+}]_{out}$ ($n = 12$); 1 mM $[Ca^{2+}]_{out}$ ($n = 12$); 1.8 mM $[Ca^{2+}]_{out}$ ($n = 12$); 5.0 mM $[Ca^{2+}]_{out}$ ($n = 12$); 10 mM $[Ca^{2+}]_{out}$ ($n = 10$); 100 nM nifedipine in the presence of 1 mM $[Ca^{2+}]_{out}$ ($n = 10$); 1 μM NPS2143 in the presence of 5.0 mM $[Ca^{2+}]_{out}$ ($n = 6$); 1 nM U-73343 in the presence of 5.0 mM $[Ca^{2+}]_{out}$ ($n = 5$); and 1 nM U-73122 in the presence of 5.0 mM $[Ca^{2+}]_{out}$ ($n = 5$). Vertical bars indicate the means ± standard deviations. * $P < 0.05$.

highest at this calcium concentration (Fig. 2Ca, Cb).

Since an elevation of $[Ca^{2+}]_{out}$ to 5 mM resulted in greater expression of BMP-2 mRNA and protein (Fig. 2Ca, Cb) as well as a rise in $[Ca^{2+}]_{in}$ that was blunted by PLC inhibition (Fig. 3), next we investigated the effects of PLC on the production of BMP-2 using U-73122 as a pharmacologic inhibitor of PLC and U-73343 as a control. The expression of BMP-2 mRNA was not increased in hASCs cultured in the presence of 1 nM U-73122 (Fig. 4Aa): 1.00 ± 0.06-fold at 0 h (control; $n = 4$); 1.07 ± 0.08-fold at 24 h ($n = 4$); and 0.99 ± 0.05-fold at 48 h ($n = 4$). This contrasted with the increase in BMP-2 mRNA detected after 48 h of culture in 5 mM $[Ca^{2+}]_{out}$ in the absence of the PLC inhibitor (Fig. 2Ca). Furthermore, the level of BMP-2 protein in hASCs cultured for 48 h was significantly decreased by U-73122 (Fig. 4Ab) from 48.3 ± 5.8 pg/mL ($n = 3$) in the absence of U-73122 to 25.0 ± 8.7 pg/mL ($n = 3$) in its presence ($P = 0.023$). By contrast, the expression of BMP-2 mRNA in the presence of 1 nM U-73343 (control) showed a time-dependent increase up to 48 h (Fig. 4Ba): 1.0 ± 0.06-fold at 0 h (control; $n = 4$); 1.4 ± 0.08-fold at 24 h ($n = 4$); and 1.5 ± 0.013-fold at 48 h ($n = 4$). In addition, the protein level of BMP-2 in hASCs cultured for 48 h was not affected by 1 nM U-73343 (48.3 ± 5.8 pg/mL in the control, $n = 4$; and 46.7 ± 7.6 pg/mL in the presence of U-73122, $n = 3$; Fig. 4Bb). Thus, PLC inhibition attenuated the levels of BNP-2 mRNA and protein in hASCs, consistent with its effects on $[Ca^{2+}]_{in}$.

Next, the influence of calmodulin on the production of BMP-2 was investigated using the calmodulin antagonist, W-7. The expression of BMP-2 mRNA showed a significant time-dependent decrease in hASCs cultured in the presence of 10 nM W-7 (Fig. 4Ca): 1.00 ± 0.06-fold at 0 h (control; $n = 4$); 0.92 ± 0.08-fold at 24 h ($n = 4$); and 0.70 ± 0.10-fold at 48 h ($n = 4$). The protein level of BMP-2 was also decreased by 10 nM W-7 in hASCs cultured for 48 h (48.3 ± 5.8 pg/mL for the control, $n = 4$; and 23.4 ± 12.6 pg/mL in the presence of W-7, $n = 4$; $P = 0.004$; Fig. 4Cb).

To further explore the mechanisms regulating the production of BMP-2 in hASCs, the possible influence of NFAT on BMP-2 levels was investigated using the NFAT inhibitor, 11R-VIVIT. The expression of BMP-2 mRNA showed a significant time-dependent decrease in hASCs cultured in the presence of 1 μM 11R-VIVIT (Fig. 4Da): 1.00 ± 0.08-fold at 0 h (control; $n = 4$); 0.84 ± 0.03-fold at 24 h ($n = 4$); and 0.64 ± 0.05-fold at 48 h ($n = 4$). The protein level of BMP-2 was also decreased by 1 μM 11R-VIVIT in hASCs cultured for 48 h (48.3 ± 7.6pg/mL for the control, $n = 4$; and 18.3 ± 5.7 pg/mL in the presence of 11R-VIVIT, $n = 4$; $P = 0.012$; Fig. 4Db).

Next, the effects of PLC on calcineurin expression were investigated using U-73122 as a pharmacologic inhibitor of PLC and U-73343 as a control. The expression of calcineurin mRNA exhibited a time-dependent increase in hASCs cultured in 5.0 mM $[Ca^{2+}]_{out}$ (Fig. 4Ea): 1.00 ± 0.06-fold at 0 h (control; $n = 4$); 1.80 ± 0.03-fold at 24 h ($n = 4$, $P = 0.004$); and 2.70 ± 0.05-fold at 48 h ($n = 4$, $P = 0.0001$). A similar time-dependent increase in calcineurin mRNA level was observed in cells cultured in the presence of 1 nM U-73343 at 5.0 mM $[Ca^{2+}]_{out}$ (Fig. 4Ec): 1.00 ± 0.06-fold at 0 h (control; $n = 4$); 1.60 ± 0.10-fold at 24 h ($n = 4$, $P = 0.006$); and 2.50 ± 0.05-fold at 48 h ($n = 4$, $P = 0.005$). By contrast, the expression of calcineurin mRNA showed little change in hASCs cultured in the presence of 1 nM U-73122 (Fig. 4Eb): 1.00 ± 0.06-fold at 0 h (control; $n = 4$); 1.10 ± 0.10-fold at 24 h ($n = 4$); and 1.13 ± 0.06-fold at 48 h ($n = 4$).

Intracellular Ca^{2+} binds to calmodulin and then activates the calcineurin/NFAT pathway, which leads to the production of BMP-2. Therefore, we carried out western blotting experiments to determine the effects of $[Ca^{2+}]_{out}$ on the translocation of dephosphorylated NFAT2 to the nucleus in hASCs. When hASCs were cultured in ODM containing 5.0 mM $[Ca^{2+}]_{out}$ for 48 h, the cytoplasmic level of phosphorylated NFAT2 decreased in a time-dependent manner (Fig. 4Fa), while the nuclear fraction of phosphorylated NFAT2 gradually increased over 48 h (Fig. 4Fb).

4. Discussion

In the present study, we demonstrated that rhBMP-2 as well as extracellular calcium stimulated the differentiation of hASCs into osteogenic cells *via* activation of the CaSR and recruitment of Ca^{2+}/calmodulin-dependent NFAT-signaling pathways.

In previous experiments (data not shown), we confirmed that cells isolated from human abdominal fat tissue are positive for markers of mesenchymal stem cells (CD73, CD90 and CD105) and negative for markers of hematopoietic stem cells (CD14, CD34 and CD45) [32]. Therefore, the cells used in this study were ASCs.

Runx2 is a transcription factor involved in osteoblastic differentiation and skeletal morphogenesis and is expressed during the early stage of osteoblastic differentiation [24]. Runx2 regulates osterix expression by binding to its promoter [22]. Osterix is also a zinc finger-containing transcription factor required for osteoblast differentiation and bone formation [23]. Conversely, osteonectin is expressed at a later stage of differentiation [25]. Both BSP (an acidic, noncollagenous glycoprotein) and osteocalcin (a bone Gla protein) are expressed in osteoblasts [26]. BMP-2 has been shown to stimulate osteogenic differentiation in mesenchymal progenitor cells [9,33] and activate the transdifferentiation of non-osteogenic mesenchymal cells, including ASCs, to osteogenic cells [12,34,35]. Thus, we investigated the temporal expression profiles of osteogenic differentiation determinants at various time points after the exposure of hASCs to ODM. In agreement with previous reports [9,12,22,23,33–35], stimulation with rhBMP-2 significantly increased Runx2 mRNA expression at day 3 and osterix mRNA expression at day 10 (Fig. 1E). rhBMP-2 also enhanced the mRNA expressions of

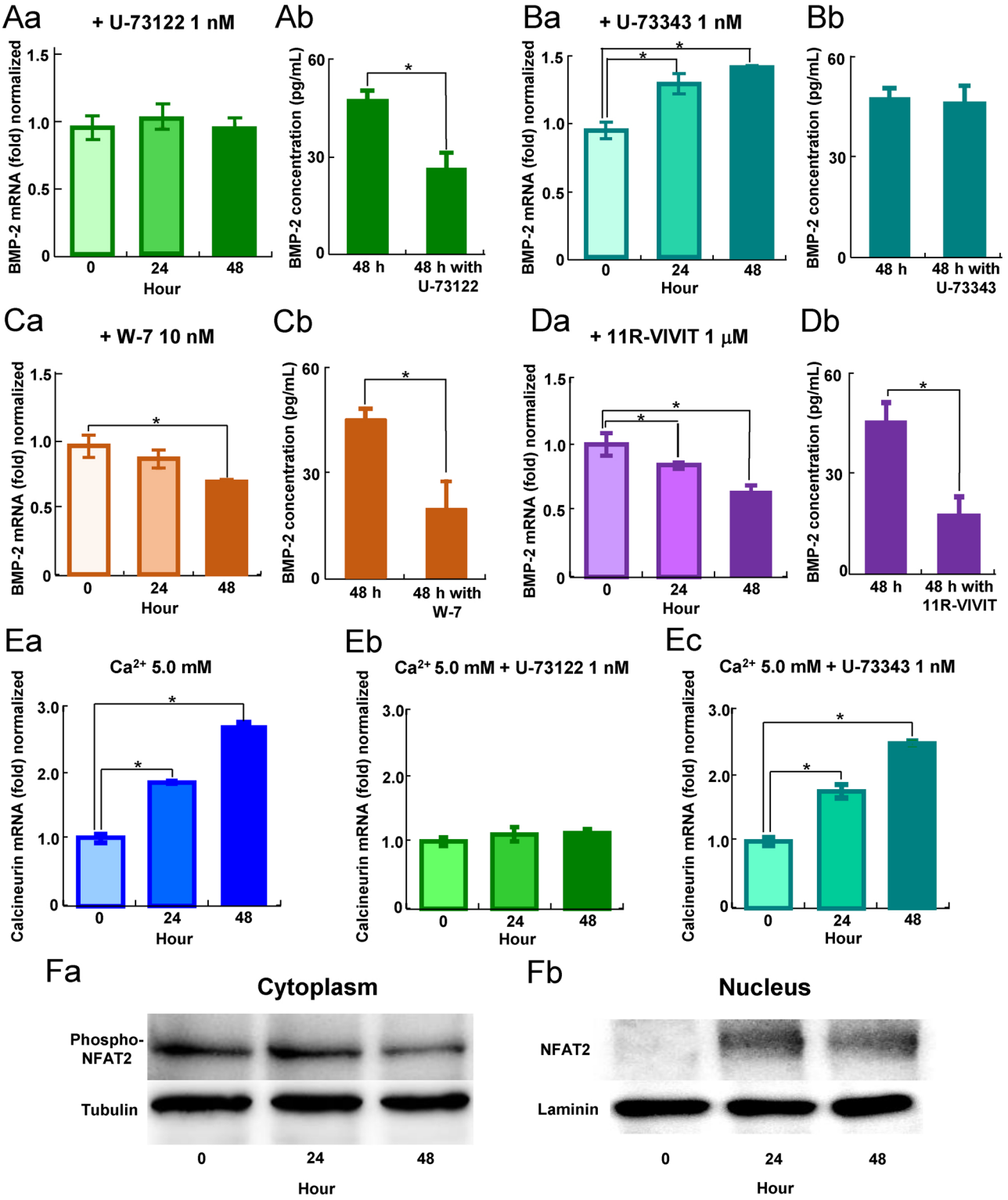

Fig. 4. The roles of calmodulin and nuclear factor of activated T-cells (NFAT) signaling in the effects of extracellular calcium ion concentration ($[Ca^{2+}]_{out}$) on bone morphogenetic protein-2 (BMP-2) levels in human adipose-derived stem cells (hASCs).
(A–D) hASCs were cultured in osteogenic differentiation medium containing 5.0 mM Ca^{2+} in the presence of 1 nM U-73122 (a phospholipase C inhibitor; **Aa**, **Ab**), 1 nM U-73343 (an inactive analogue of U73122; **Ba**, **Bb**), 10 nM W-7 (a calmodulin antagonist: **Ca** and **Cb**) or 1 μM 11R-VIVIT (a NFAT inhibitor; **Da**, **Db**) for 24 or 48 h. BMP-2 mRNA expression was determined using real-time polymerase chain reaction (**Aa**, **Ba**, **Ca**, **Da**). The BMP-2 mRNA levels were normalized to that of β-actin and expressed relative to that in unstimulated cells in medium containing 0.3 mM Ca^{2+} at day 0. BMP-2 protein levels were determined using an enzyme-linked immunosorbent assay kit (**Ab**, **Bb**, **Cb**, **Db**). Vertical bars indicate the means ± standard deviations ($n = 4$). * $P < 0.05$. **(E)** hASCs were cultured for 24 or 48 h in osteogenic differentiation medium containing 5.0 mM $[Ca^{2+}]_{out}$ (**Ea**) and the effects of U-73122 (**Eb**) and U-73343 (**Ec**) were evaluated. Calcineurin mRNA expression was determined using real-time polymerase chain reaction. The calcineurin mRNA levels were normalized to that of β-actin and expressed relative to that in unstimulated cells in medium containing 0.3 mM Ca^{2+} at day 0. **(F)** Cytoplasmic fractions of phosphorylated NFAT2 (phospho-NFAT2) and tubulin (internal control) and nuclear fractions of NFAT2 and laminin (internal control) in hASCs cultured for 24 or 48 h in osteogenic differentiation medium containing 5.0 mM $[Ca^{2+}]_{out}$. The experiments were carried out using the western blot technique.

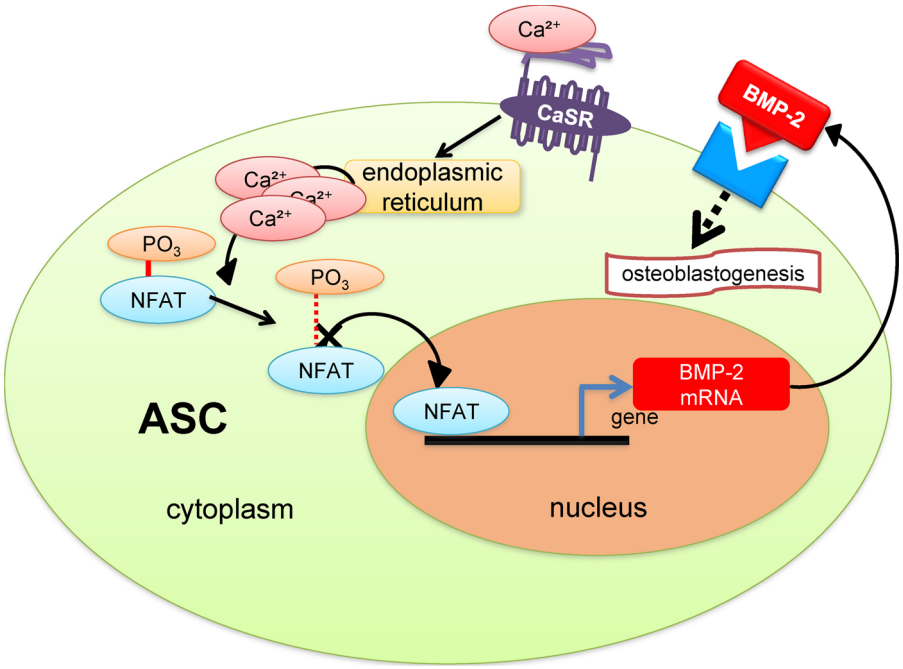

Fig. 5. Schematic diagram illustrating the possible mechanisms involved in the differentiation of adipose-derived stem cells (ASCs) to osteoblasts.
An elevation of extracellular calcium concentration activates the calcium-sensing receptor (CaSR) to induce Ca^{2+}-release from intracellular Ca^{2+} stores. The resulting rise in intracellular Ca^{2+} increases the binding of Ca^{2+} to calmodulin. The Ca^{2+}-calmodulin complex promotes dephosphorylation of cytoplasmic phosphorylated nuclear factor of activated T-cells (NFAT2). This allows NFAT2 to migrate into the nucleus and activate the transcription of bone morphogenetic protein-2 (BMP-2) mRNA, leading to an increase in the BMP-2 protein level.

osteonectin, BSP and osteocalcin at day 10 (Fig. 1E). Furthermore, Alizarin red and von Kossa staining of hASCs revealed that rhBMP-2 enhanced calcium deposition and mineralization (Fig. 1A–C). These results strongly suggest that rhBMP-2 promotes the differentiation of hASCs to osteogenic cells and mineralization.

In this study, we used an increase in $[Ca^{2+}]_{out}$ as an alternative method of priming the differentiation process. Higher $[Ca^{2+}]_{out}$ promoted the mRNA expressions of Runx2, ALP and osteocalcin (Fig. 2A, 2B) similar to that seen in response to rhBMP-2, indicating that elevated $[Ca^{2+}]_{out}$ can enhance the expressions of genes associated with osteogenic differentiation. Increasing $[Ca^{2+}]_{out}$ levels resulted in a transient elevation of $[Ca^{2+}]_{in}$, suggesting that the rise in $[Ca^{2+}]_{in}$ was likely not due to diffuse Ca^{2+} entry into the hASCs.

$[Ca^{2+}]_{in}$ can be increased by the action of growth factors/cytokines, ion channels and biological processes such as the assembly and dissociation of cell-cell contacts or cell-cell matrix contacts [36]. A previous study reported that voltage-gated calcium channels are potential candidates as regulators of bone cell metabolism in MC3T3-E1 osteoblasts [37]. However, voltage-gated calcium channels are unlikely to play a role in the osteogenic differentiation of hASCs because, in our experiments, nifedipine (a well-known and potent antagonist of voltage-gated Ca^{2+} channels) enhanced Ca^{2+} influx rather than inhibited it, leading to an increase in the production of BMP-2 (Figs. 2F, 3 Ca & E).

The CaSR is a seven-transmembrane, GTP-binding, protein-coupled receptor expressed in various cell types, including osteoblasts [38]. A previous investigation showed that the CaSR might be a physiological regulator of bone cell metabolism [39]. Based on the results of the present study, the CaSR is the most promising mechanism underlying the rise in $[Ca^{2+}]_{in}$ in response to an increase in $[Ca^{2+}]_{out}$ in hASCs. This is because nifedipine, a reported agonist of the CaSR [37], enhanced Ca^{2+} influx and increased the production of BMP-2 in hASCs. Furthermore, another CaSR agonist, R568, also increased the production of BMP-2, whereas a CaSR antagonist, NPS2143, decreased not only $[Ca^{2+}]_{in}$ but also the production of BMP-2 (Figs. 2F, 3 Ca, Cb & E). The production of BMP-2 by human colon myofibroblasts expressing the CaSR has been reported to be dependent on $[Ca^{2+}]_{out}$ *via* a mechanism involving the CaSR [40]. Moreover, we have also observed BMP-2 production that is dependent on $[Ca^{2+}]_{out}$ in keratocystic odontogenic tumor-derived and gingival-derived human fibroblasts expressing the CaSR.

It was notable that hASCs cultured in ODM containing no BMP-2 and 0.3 mM $[Ca^{2+}]_{out}$ exhibited increased expression of Runx2 on day 3 (Fig. 2Ba). Therefore, it is likely that factors other than BMP-2 and calcium are involved in the expression of Runx2, and further studies will be needed to identify these factors. Nonetheless, it is evident from our experimental results that CaSR mRNA expression tended to increase on day 3 when $[Ca^{2+}]_{out}$ was elevated to 1.8 mM (2.09 ± 0.30-fold) or 5.0 mM (3.89 ± 0.28-fold; Fig. 2E) and that the expression of Runx2 mRNA was also enhanced by 5.0 mM $[Ca^{2+}]_{out}$ on day 3 (Fig. 2Ba). Thus, when taken together with the observation that an elevation of $[Ca^{2+}]_{out}$ to 5.0 mM elicited a large and rapid increase in BMP-2 expression within 24 h (Fig. 2Ca), the increased mRNA expression of Runx2 on day 3 would not be inconsistent with the time course of the upregulation of CaSR mRNA expression after a rise in $[Ca^{2+}]_{out}$.

An elevation of $[Ca^{2+}]_{in}$ will enhance the binding of Ca^{2+} to calmodulin and induce the dephosphorylation of NFAT through the activation of calcineurin; dephosphorylated NFAT may then translocate to the nucleus [15]. In our study, U-73122 attenuated the increases in $[Ca^{2+}]_{in}$ and calcineurin mRNA expression in response to a rise in $[Ca^{2+}]_{out}$ (Figs. 3D, E & 4 E), indicating that PLC is involved in the elevation of $[Ca^{2+}]_{in}$ and activation of calcineurin induced by an increase in $[Ca^{2+}]_{out}$. We suggest that this elevation in $[Ca^{2+}]_{in}$ acts *via* a calcium-calmodulin complex (Ca/CaM) to induce the dephosphorylation of NFAT and thus activation of BMP-2 gene expression. This involvement of the Ca/CaM/NFAT pathway is supported by the observations that the Ca/CaM inhibitor, W-7, and the NFAT inhibitor, 11R-VIVIT, attenuated the levels of BMP-2 mRNA and protein (Fig. 4C & D). Moreover, an increase in $[Ca^{2+}]_{out}$ activated ALP in a concentration-dependent manner (Fig. 2Ab), suggesting that the BMP-2 produced in response to a rise in $[Ca^{2+}]_{out}$ induced the osteogenic differentiation of hASCs. Although both U-73122 and W-7 lowered the protein level of BMP-2, it was notable that BMP-2 mRNA expression was suppressed only by W-7 and not by U-73122 (Fig. 4A & C). A possible explanation for this apparent discrepancy is that the expression levels of mRNA and protein do no always change in parallel (a widely recognized phenomenon). It is likely that PLC inhibition may have affected the synthesis of BMP-2 protein as well as the expression of BMP-2 mRNA, since the PLC pathway involves many intracellular signaling cascades.

BMP-2 has been reported to activate osteoclastogenesis [41], while active NFAT2 has been shown to stimulate osteoclastic differentiation of a monocyte line [42]. However, in the present study, hASCs did not differentiate into osteoclasts even in the presence of rhBMP-2, which was confirmed by tartrate-resistant acid phosphatase staining (data not shown). This suggests that the sensitivity to BMP-2 differs among cell types, since the balance between osteoclastogenesis and osteoblastogenesis is regulated by the BMP-2 concentration [37].

In summary, our findings demonstrate that osteogenic differentiation of hASCs was activated by rhBMP-2. Furthermore, an increase in $[Ca^{2+}]_{out}$ resulted in an elevation of $[Ca^{2+}]_{in}$ due to activation of the CaSR. Importantly, the expression of BMP-2 was enhanced by an elevation of $[Ca^{2+}]_{out}$ *via* activation of the CaSR and recruitment of Ca^{2+}/calmodulin-dependent NFAT-signaling pathways (Fig. 5). Therefore, an increase in extracellular calcium might induce osteogenic differentiation of hASCs by autocrine and/or paracrine signaling. These findings suggest that the administration of calcium may be an alternative or adjuvant method to BMP-2 for inducing the osteogenic differentiation of hASCs *in vitro*.

Author's contributions

Conception and design: R.Y., S.K., S.I., M.I.
Financial support: Y.K., S.K.
Administrative support: Y.K., Y.M.
Provision of study material or patients: R.Y., F.T., S.K., S.I., M.I.
Collection and/or assembly of data: R.Y., T.M., S.K.
Data analysis and interpretation: R.Y., F.T., S.K., S.I., M.I., T.M. *J*.Y.
Manuscript writing: Y.K., S.K., R.Y., T.M., *J*.Y.
Final approval of manuscript: Y.M., S.K.
Other (please be specific): none.

Disclosure of Potential Conflicts of Interest

None.

Acknowledgements

This work was supported by a Grant-Aid for Special Purpose (No. 25463088) from the Japan Society for the Promotion of Science. We also thank www.oxmedcomms.com for writing assistance.

References

[1] P.A. Zuk, M. Zhu, P. Ashjian, et al., Human adipose tissue is a source of multipotent stem cells, Mol. Biol. Cell 13 (2002) 4279–4295.
[2] B.A. Bunnell, M. Flaat, C. Gagliardi, et al., Adipose-derived stem cells: isolation, expansion and differentiation, Methods 45 (2008) 115–120.
[3] M.F. Pittenger, A.M. Mackay, S.C. Beck, et al., Multilineage potential of adult human mesenchymal stem cells, Science 284 (1999) 143–147.
[4] K. Mesimäki, B. Lindroos, J. Törnwall, et al., Novel maxillary reconstruction with ectopic bone formation by GMP adipose stem cells, Int. J. Oral Maxillofac. Surg. 38 (2009) 201–209.
[5] M. Jäger, E.M. Jelinek, K.M. Wess, et al., Bone marrow concentrate: a novel strategy for bone defect treatment, Curr. Stem Cell Res. Ther. 4 (2009) 34–43.
[6] U. Nöth, A.M. Osyczka, R. Tuli, et al., Multilineage mesenchymal differentiation potential of human trabecular bone-derived cells, J. Orthop. Res. 20 (2002) 1060–1069.
[7] B.L. Hogan, Bone morphogenetic proteins in development, Curr. Opin. Genet. Dev. 6 (1996) 432–438.
[8] E.H.J. Groeneveld, E.H. Burger, Bone morphogenetic proteins in human bone regeneration, Eur. J. Endocr. Med. 142 (2000) 9–21.
[9] H. Hu, M.J. Hilton, X. Tu, et al., Sequential roles of Hedgehog and Wnt signaling in osteoblast development, Development 132 (2005) 49–60.
[10] H.M. Ryoo, M.H. Lee, Y.J. Kim, Critical molecular switches involved in BMP-2-induced osteogenic differentiation of mesenchymal cells, Gene 366 (2006) 51–57.
[11] K. Umehara, T. Iimura, K. Sakamoto, et al., Canine oral mucosal fibroblasts differentiate into osteoblastic cells in response to BMP-2, Anat. Rec. (Hoboken) 295 (2012) 1327–1335.
[12] N. Quarto, M.T. Longaker, Differential expression of specific FGF ligands and receptor isoforms during osteogenic differentiation of mouse adipose-derived stem cells (mASCs) recapitulates the in vivo osteogenic pattern, Gene 424 (2008) 130–140.
[13] M.A. Valdes, N.A. Thakur, S. Namdari, D.M. Ciombor, M. Palumbo, Recombinant bone morphogenic protein-2 in orthopaedic surgery: a review, Arch. Orthop. Trauma Surg. 129 (2009) 1651–1657.
[14] M.J. Berridge, P. Lipp, M.D. Bootman, The versatility and universality of calcium signalling, Nat. Rev. Mol. Cell Biol. 1 (2000) 11–21.
[15] J. Aramburu, A. Rao, C.B. Klee, Calcineurin: from structure to function, Curr. Top. Cell. Regul. 36 (2000) 237–295.
[16] D.A. Rider, T. Nalathamby, V. Nurcombe, et al., Selection using the alpha-1 integrin (CD49a) enhances the multipotentiality of the mesenchymal stem cell population from heterogeneous bone marrow stromal cells, J. Mol. Histol. 38 (2007) 449–458.
[17] W.M. Flanagan, B. Corthesy, R.J. Bram, et al., Nuclear association of a T-cell transcription factor blocked by FK-506 and cyclosporin A, Nature 352 (1991) 803–807.
[18] J.D. Molkentin, J.R. Lu, C.L. Antos, et al., A calcineurin-dependent transcriptional pathway for cardiac hypertrophy, Cell 93 (1998) 215–228.
[19] M.M. Winslow, M. Pan, M. Starbuck, et al., Calcineurin/NFAT signaling in osteoblasts regulates bone mass, Dev. Cell 10 (2006) 771–782.
[20] M. Tomita, M.I. Reinhold, J.D. Molkentin, et al., Calcineurin and NFAT4 induce chondrogenesis, J. Biol. Chem. 277 (2002) 42214–42218.
[21] S. Ogata, Y. Kubota, S. Satoh, et al., Ca^{2+} stimulates COX-2 expression through calcium-sensing receptor in fibroblasts, Biochem. Biophys. Res. Commun. 351 (2006) 808–814.
[22] T. Matsubara, K. Kida, A. Yamaguchi, et al., BMP2 regulates Osterix through Msx2 and Runx2 during osteoblast differentiation, J. Biol. Chem. 28 (2008) 29119–29125.
[23] K. Nakashima, X. Zhou, G. Kunkel, et al., The novel zinc finger-containing transcription factor osterix is required for osteoblast differentiation and bone formation, Cell 108 (2002) 17–29.
[24] J.H. Jonason, G. Xiao, M. Zhang, L. Xing, D. Chen, Post-translational regulation of Runx2 in bone and cartilage, J. Dent. Res. 88 (2009) 693–703.
[25] M.W. Long, Osteogenesis and bone marrow-derived cells, Blood Cells Mol. Dis. 2 (2001) 677–690.
[26] R. Fujisawa, M. Tamura, Acidic bone matrix proteins and their roles in calcification, Front. Biosci. (Landmark Ed) 17 (2012) 1891–1903.
[27] N. Griesche, W. Luttmann, A. Luttmann, et al., A simple modification of the separation method reduces heterogeneity of adipose-derived stem cells, Cells Tissues Organs 192 (2010) 106–115.
[28] E. Arrigoni, S. Lopa, L. de Girolamo, et al., Isolation, characterization and osteogenic differentiation of adipose-derived stem cells: from small to large animal models, Cell Tissue Res. 338 (2009) 401–411.
[29] C.A. Schneider, W.S. Rasband, K.W. Eliceiri, NIH Image to ImageJ: 25 years of image analysis, Nat. Methods 9 (2012) 671–675.
[30] Z.H. Fei, C.Y. Yao, X.L. Yang, et al., Serum BMP-2 up-regulation as an indicator of poor survival in advanced non-small cell lung cancer patients, Asian Pac. J. Cancer Prev. 14 (2013) 5293–5299.
[31] A.M. Barradas, H.A. Fernandes, N. Groen, et al., A calcium-induced signaling cascade leading to osteogenic differentiation of human bone marrow-derived mesenchymal stromal cells, Biomaterials 33 (2012) 3205–3215.
[32] H.H. Lin, S.M. Hwang, S.J. Wu, et al., The osteoblastogenesis potential of adipose mesenchymal stem cells in myeloma patients who had received intensive therapy, PLoS One 9 (4) (2014) e94395.
[33] T.F. Day, X. Guo, L. Garrett-Beal, et al., Wnt/beta-catenin signaling in mesenchymal progenitors controls osteoblast and chondrocyte differentiation during vertebrate skeletogenesis, Dev. Cell 8 (2005) 739–750.
[34] D.C. Wan, Y.Y. Shi, R.P. Nacamuli, et al., Osteogenic differentiation of mouse adipose-derived adult stromal cells requires retinoic acid and bone morphogenetic protein receptor type IB signaling, Proc. Natl. Acad. Sci. U. S. A. 103 (2006) 12335–12340.
[35] N.J. Panetta, D.M. Gupta, J.K. Lee, et al., Human adipose-derived stromal cells respond to and elaborate bone morphogenetic protein-2 during in vitro osteogenic differentiation, Plast. Reconstr. Surg. 125 (2010) 483–493.
[36] K.A. Fagan, R.A. Graf, S. Tolman, et al., Regulation of Ca^{2+}-sensitive adenylyl cyclase in an excitable cell, J. Biol. Chem. 275 (2000) 40187–40194.
[37] X. Sun, V. Kishore, K. Fites, et al., Osteoblasts detect pericellular calcium concentration increase via neomycin-sensitive voltage gated calcium channels, Bone 51 (2012) 860–867.
[38] T.I. Alfadda, A.M. Saleh, P. Houillier, J.P. Geibel, Calcium-sensing receptor 20 years later, Am. J. Physiol. Cell Physiol. 307 (2014) C221–231.
[39] P.J. Marie, The calcium-sensing receptor in bone cells: a potential therapeutic target in osteoporosis, Bone 46 (2010) 571–576.
[40] D. Peiris, I. Pacheco, C. Spencer, et al., The extracellular calcium-sensing receptor reciprocally regulates the secretion of BMP-2 and the BMP antagonist Noggin in colonic myofibroblasts, Am. J. Physiol. Gastrointest. Liver Physiol. 292 (3) (2007) G753–766.
[41] R.Y. Kim, J.H. Oh, B.S. Lee, et al., The effect of dose on rhBMP-2 signaling, delivered via collagen sponge, on osteoclast activation and in vivo bone resorption, Biomaterials 35 (2014) 1869–1881.
[42] H. Hirotani, N.A. Tuohy, J.T. Woo, et al., The calcineurin/nuclear factor of activated T cells signaling pathway regulates osteoclastogenesis in RAW264.7 cells, J. Biol. Chem. 279 (2004) 13984–13992.